Nanoparticle Self-Assembly

DOI: 10.1002/anie.201406323

Polyrotaxane-Mediated Self-Assembly of Gold Nanospheres into Fully Reversible Supercrystals**

*Joao Paulo Coelho, Guillermo González-Rubio, Annette Delices, José Osío Barcina, Cástor Salgado, David Ávila, Ovidio Peña-Rodríguez, Gloria Tardajos, and Andrés Guerrero-Martínez**

Abstract: *The use of a thiol-functionalized nonionic surfactant to stabilize spherical gold nanoparticles in water induces the spontaneous formation of polyrotaxanes at the nanoparticle surface in the presence of the macrocycle α-cyclodextrin. Whereas using an excess of surfactant an amorphous gold nanocomposite is obtained, under controlled drying conditions the self-assembly between the surface supramolecules provides large and homogenous supercrystals with hexagonal close packing of nanoparticles. Once formed, the self-assembled supercrystals can be fully redispersed in water. The reversibility of the crystallization process may offer an excellent reusable material to prepare gold nanoparticle inks and optical sensors with the potential to be recovered after use.*

In recent years, supramolecular chemistry has focused on the organization of molecular systems in the solid state and/or at solid–liquid interfaces,[1] in analogy to what has been previously done at the molecular level in solution, to develop new functional materials.[2] Of particular interest are arrangements of supramolecules on the surface of inorganic nanoparticles,[3] with the aim that self-assembly should occur to form nanostructures that are able to perform functions not present in their individual components.[4] However, control of supramolecular self-assembly to produce large arrays with defined geometrical arrangements of the nanoparticles remains a difficult task.[5] Within this context, plasmonic metal nanoparticles coated with rationally selected organic molecules and biomolecules have been arranged to build up plasmonic dimers, polymers, and supercrystals,[6] showing interesting collective optical and sensing responses.[7]

One of the most appealing families of supramolecules because of simplicity in their chemical synthesis are cyclodextrin (CD) polyrotaxanes,[8] in which several CD macrocycles are entrapped by a molecular axis without bulky end groups. From the first report describing the preparation of a polyrotaxane-based solid complex between α-CD (six α-D-(+)-glucopyranose units) and polyethylene glycol,[9a] many of these architectures have been synthesized using different CDs and polymers.[9] In all cases, both host–guest noncovalent interactions and cooperative hydrogen bonds between the macrocycles contribute to the stability of the resulting products.[10] In this context, nonionic Igepal (polyoxyethyelene nonyl phenyl ether) surfactants have emerged as excellent candidates to prepare solid structures of self-assembled polyrotaxanes in the presence of CDs.[11a]

Herein, we demonstrate the use of CD polyrotaxanes to create supercrystals of highly ordered supramolecularly stabilized spherical gold nanocrystals, which exhibit reversible crystallization (Scheme 1). The supramolecules were prepared in water by α-CD complexation of a new thiol-functionalized Igepal surfactant IgeSH (Scheme 1; see Supporting Information for synthesis and characterization) which stabilizes the surface of the nanocrystals. The choice of the Igepal as capping agent is dictated by its high tendency to form CD polyrotaxanes,[11] the luminescent properties of such amphiphiles and their CD complexes,[11b] and the versatility that commercially available Igepal surfactants have shown as stabilizers of metal nanoparticles.[12]

An inclusion complex was formed between α-CD and IgeSH by mixing both compounds in water (Figure 1a, and see the Supporting Information). The cloudiness of the IgeSH solution, which is related to the presence of large micelles,[13] decreased remarkably because of the disruption of aggregates by CD complexation. After 24 hours, a white powder is obtained (Figure 1a). The powder was analyzed by X-ray powder diffraction (XRPD, see Supporting Information) and transmission electron microscopy (TEM, Figure 1b). The amorphous nature of the solid indicates a random arrangement of the complexes within the precipitate. The stoichiometry of the polyrotaxane has been determined by ^{1}H NMR spectroscopy (Supporting Information), showing the formation of IgeSH:CD complexes in a 1:4 ratio. The assembly and precipitation of such supramolecules is driven by strong

[*] J. P. Coelho, G. González-Rubio, A. Delices, Prof. G. Tardajos, Dr. A. Guerrero-Martínez
Departamento de Química Física I
Universidad Complutense de Madrid
Avda. Complutense s/n, 28040, Madrid (Spain)
E-mail: aguerrero@quim.ucm.es
Prof. J. O. Barcina, C. Salgado
Departamento de Química Orgánica I
Universidad Complutense de Madrid
Avda. Complutense s/n, 28040, Madrid (Spain)
Dr. D. Ávila
Departamento de Química Inorgánica
Universidad Complutense de Madrid
Avda. Complutense s/n, 28040, Madrid (Spain)
Dr. O. Peña-Rodríguez
Instituto de Fusión Nuclear, Universidad Politécnica de Madrid
José Gutiérrez Abascal 2, 28006, Madrid (Spain)

[**] This work has been funded by the Spanish MINECO (CTQ2010-18564). J.P.C. acknowledges receipt of a Ciências sem Fronteiras fellowship from the CNPq of Brazil. A.G.-M. acknowledges receipt of a Ramón y Cajal Fellowship from the Spanish MINECO.

Supporting information for this article is available on the WWW under http://dx.doi.org/10.1002/anie.201406323.

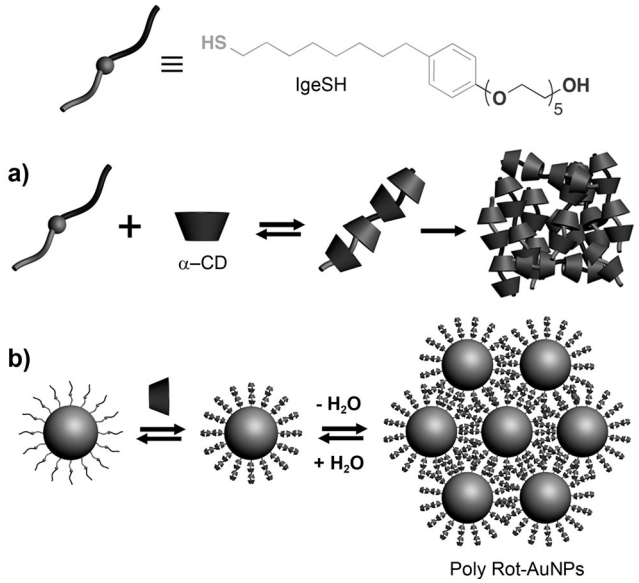

Scheme 1. Chemical structure of the nonionic Igepal surfactant IgeSH with hydrophobic (gray) and hydrophilic (black) regions. a) Preparation of the amorphous nonreversible solid network of polyrotaxanes with IgeSH and α-CD in water. b) Preparation of the reversible supercrystals of polyrotaxane-stabilized spherical gold nanoparticles (PolyRot-AuNPs) in water.

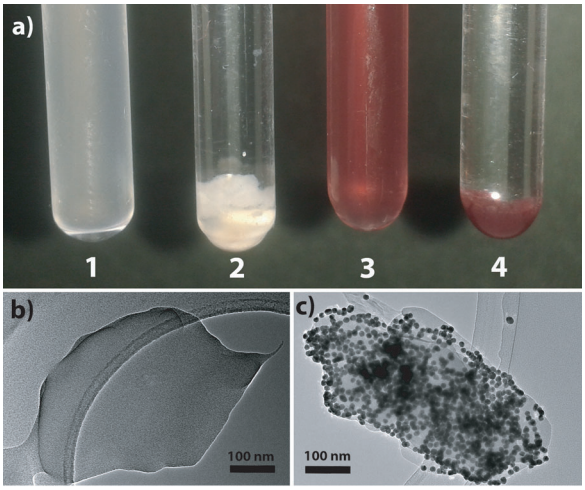

Figure 1. a) Evolution of a cloudy solution of IgeSH (1 mM) in the absence (1) and the presence (2) of α-CD (10 mM) after 24 hours. Evolution of the same solutions of IgeSH with added IgeS-AuNPs (4×10^{-9} M), in the absence (3) and the presence (4) of α-CD. b) TEM micrograph of the amorphous polyrotaxane solid obtained in (2). c) TEM micrograph of the gold nanocrystalline nanocomposite obtained in (4). Scale bar in (b) and (c) = 100 nm.

intermolecular interactions because of the spatial anisotropy of their dielectric properties, reducing the hydration states of host and guest molecules.[10]

To test the ability of the polyrotaxanes to direct the self-assembly of gold nanocrystals, we synthesized monodisperse citrate-stabilized spherical gold nanoparticles (cit-AuNPs) of 16.0 ± 1.2 nm in diameter. The citrate ions were subsequently replaced in water with the IgeSH (see Supporting Information), driven by the stronger interaction of thiol groups with the gold surface. The UV/Vis absorption spectrum of the surfactant-stabilized nanospheres (IgeS-AuNPs) in aqueous solution shows two bands with maxima at $\lambda = 220$ and 278 nm which correspond to the Igepal absorption bands, and a characteristic localized surface plasmon resonance (LSPR) band at $\lambda = 524$ nm. This LSPR band is red-shifted by 7 nm compared to the initial cit-AuNPs (Figure 2a). This shift is in good agreement with an increase in the local refractive index of the gold nanospheres after IgeSH binding.[14] Similarly to the polyrotaxanes, IgeS-AuNPs in the presence of free IgeSH precipitate upon addition of α-CD (Figure 1a). After 24 hours, the resulting dehydrated red powder was characterized by XRPD (see Supporting Information) and TEM (Figure 1c), showing an amorphous nanocomposite in which nanocrystals are randomly assembled by CD complexation of the capping agents within the disordered polyrotaxane network.

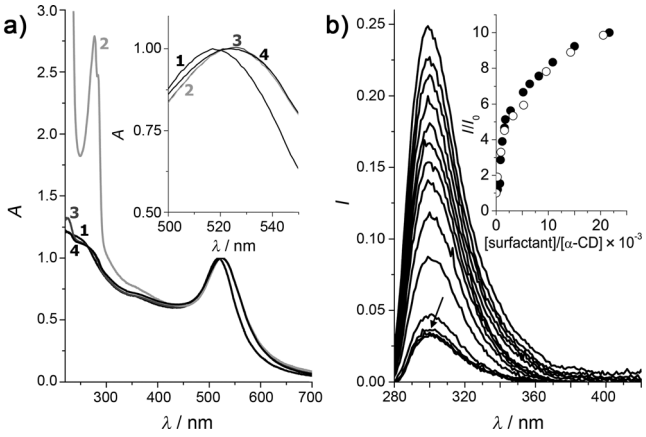

Figure 2. a) Normalized UV/Vis absorption spectra of gold nanospheres stabilized with citrate ions in aqueous solution (1), in the presence of an excess of the IgeSH surfactant (2), after removing the excess of IgeSH (3), and upon addition of α-CD (4). Inset: expanded portion of the spectrum ($\lambda = 500$–550 nm) showing the LSPR bands. b) Emission spectra of IgeS-AuNPs (2×10^{-10} M) in α-CD mixtures ($\lambda_{exc} = 220$ nm). The arrow indicates the critical concentration of α-CD (ca. 1:500 IgeS-AuNPs:α-CD) after which point the emission intensity of IgeS-AuNPs increases with increasing concentration of macrocycle. Inset: relative emission intensities versus the ratio between capping agent and α-CD (solid circles), and free IgeSH and α-CD (open circles).

The complexation process between IgeS-AuNPs and α-CD has been investigated by fluorescence measurements, upon addition of the macrocycle to a highly diluted solution of nanoparticles in which the excess of surfactant was previously removed by centrifugation (Figure 2b). The concentration of capping molecules around a nanocrystal has been estimated at approximately 5×10^3 molecules (see Supporting Information). The emission spectra exhibit a wide emission band centered at $\lambda = 300$ nm[11b] that is not quenched by the metal core (Figure 2b). Although no significant changes of the IgeS-AuNPs LSPR band have been detected upon macrocycle addition (inset in Figure 2a), an enhancement of the fluores-

cence intensity of IgeS-AuNPs has been detected (Figure 2b). This evidence suggests a stabilization of the phenyl group within the hydrophobic CD cavity, as a consequence of the dehydration of the aromatic moiety during the polyrotaxane formation. Interestingly, a critical concentration of α-CD was needed to initiate such enhancement (inset in Figure 2b; see also the Supporting Information), showing that the macrocycles are cooperatively incorporated through the oxyethylene chains until they reach the aromatic moiety. Therefore, thousands of polyrotaxanes may stabilize a unique gold nanocrystal in water (PolyRot-AuNPs, Scheme 1).

Although no crystallization has been registered between PolyRot-AuNPs in solution, even at relatively high concentrations of nanoparticles (ca. 10^{-6} M) and α-CD (solubility ca. 1.5×10^{-1} M) and with a preparation time of one month, a spontaneous formation of self-assembled layers of nanoparticles has been obtained by simple drop-casting on carbon-coated TEM grids (Figure 3; see also the Supporting Information). Whereas relatively low-ordered assemblies of IgeS-AuNPs were detected in the absence of α-CD (Figures 3a,c), well-defined islands of perfectly ordered layers of nanoparticles were formed in the presence of the macrocycle (Figure 3b). Figure 3d shows a representative TEM image of a highly ordered, bilayer array of PolyRot-AuNPs with hexagonal packing, where the octahedral and tetrahedral holes can be perfectly distinguished. The fast Fourier transform (FFT) of the image confirms a perfect hexagonal geometry, with an average distance between the centers of neighboring PolyRot-AuNPs of 19.2 nm, and a minimum distance of 3.2 nm between PolyRot-AuNPs. In the polyrotaxane structure, both the hydrophobic and hydrophilic regions of the surfactant, when completely extended with respect to the aromatic group (3.3 nm in length), are threaded by four head-to-head α-CDs (0.8 nm in height each).[15] With this structure in mind, we propose a simple molecular model in which the supramolecules self-assemble into monolayers at the surface of the nanocrystals during formation of the hexagonal superlattices (Scheme 1).

In good agreement with previous studies of AuNPs supercrystal preparation,[16] the drop-casting of cit-AuNPs and IgeS-AuNPs solutions onto quartz wafers under optimized temperature and humidity conditions (see Supporting Information), typically resulted in the formation of coffee-ring deposits of approximately 0.5 mm width and 6 mm external diameter (inset, Figure 4a), with a significant amount of inner cracks (Figures 3e,g). In contrast, a macroscopically homogenous pattern of PolyRot-AuNPs has been obtained under the same drop-casting conditions (ca. 4 mm wide, 12.6 mm^2 area; see Supporting Information). The absence of a coffee-ring deposit and the lower dimension of the PolyRot-AuNPs pattern point to strong hydrophobic interactions between nanocrystals that avoid Marangoni effects during the drying process.[17] As shown in Figures 3f and h, PolyRot-AuNPs self-assembled into supercrystals spanning approximately 4 mm in width (inset, Figure 4a) with an extraordinary long-range order. Figure 4a shows the UV/Vis absorption spectra of the different AuNP deposits upon excitation by nonpolarized irradiation perpendicularly oriented to the substrates (Supporting Information). Whereas

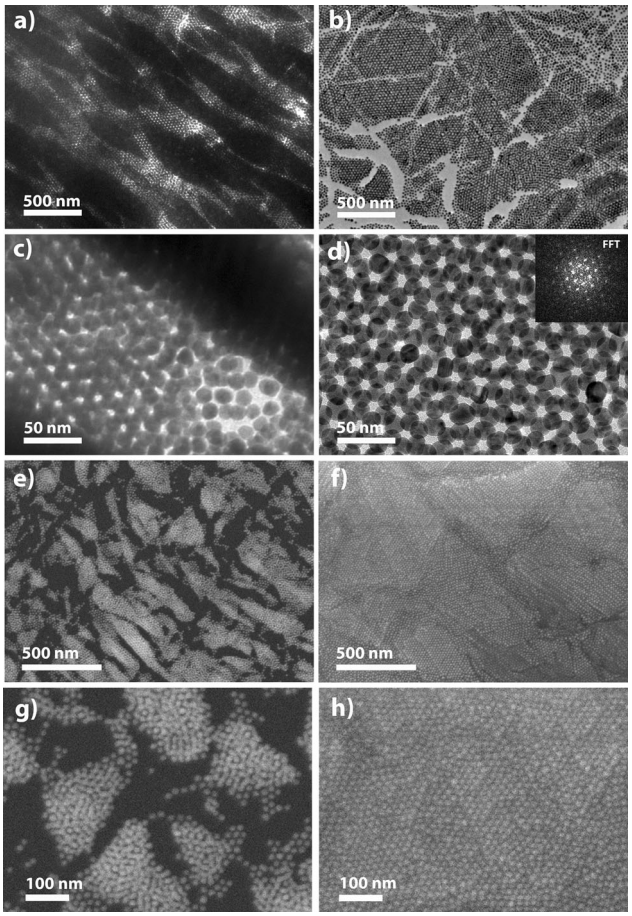

Figure 3. TEM micrographs of a) IgeS-AuNPs and b) PolyRot-AuNPs assemblies (NP concentration = 4×10^{-7} M). c) Micrograph showing the packing of IgeS-AuNPs. d) Micrograph showing a hexagonally packed bilayer of PolyRot-AuNPs and the corresponding FFT of the image (inset). Scanning electron microscopy (SEM) micrographs of e) IgeS-AuNPs and f) PolyRot-AuNPs assemblies (NP concentration = 4×10^{-7} M). g) Expanded portion of image (e) showing the packing of IgeS-AuNPs. h) Expanded portion of image (f) showing a hexagonally packed multilayer of PolyRot-AuNPs.

large broadenings of the LSPR bands occur in the case of cit-AuNPs and IgeS-AuNPs indicating low nanocrystal ordering, a narrow and intense LSPR band is obtained in the case of the PolyRot-AuNPs deposit, as a consequence of plasmon coupling between the highly ordered close-packed nanoparticles at the supercrystals (see simulated optical properties in the Supporting Information).[18] Additionally, the PolyRot-AuNPs deposit leads to highly reproducible LSPR bands within the long-range area of the substrate (Figure 4a), unlike the significant differences in the LSPR band which have been detected at the ring and center of the drop patterns of cit-AuNPs and IgeS-AuNPs. The high homogeneity of the PolyRot-AuNPs deposit may open up applications in the difficult task of imprinting metal nanoparticles from aqueous solutions.[19]

Taking into account the reversibility of supramolecular processes in solution,[20] we investigated the origin of the interactions between the self-assembled nanocrystals within

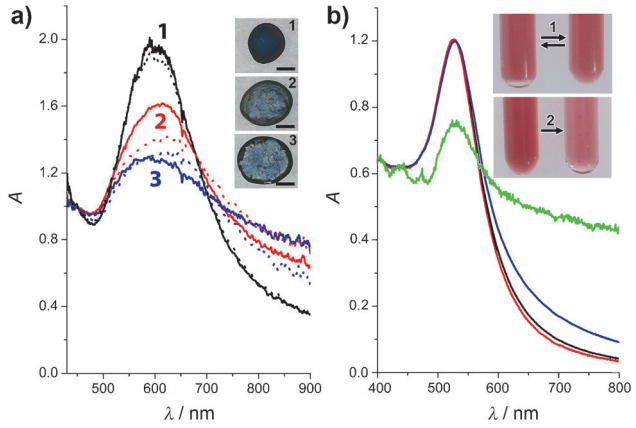

Figure 4. a) Normalized UV/Vis absorption spectra of deposits of PolyRot-AuNPs (1), IgeS-AuNPs (2), and cit-AuNPs (3), formed upon drop-casting onto a quartz wafer (10 μL volume; AuNPs concentration = 4×10^{-7} M), at the ring (solid lines) and inner (dashed lines) of the drop patterns. Inset: corresponding patterns, scale bar = 2 mm. b) Normalized UV/Vis absorption spectra of the PolyRot-AuNPs solutions before (black) and after (red) redispersion of supercrystals, and redispersed solutions of the IgeS-AuNPs (blue) and cit-AuNPs (green) deposits. Inset: redispersion of the PolyRot-AuNPs (1) and IgeS-AuNPs (2) supercrystals leads to complete (1) and partial (2) recovery of the initial colloidal solutions.

the supercrystals. Whereas no recovering of the colloid was observed by redispersion of the cit-AuNPs deposits in water, the redispersion of IgeS-AuNPs and PolyRot-AuNPs supercrystals leads to a partial and complete recovery of the initial colloidal solutions, respectively (inset, Figure 4b). The full reversibility of the interactions between polyrotaxanes at the surface of PolyRot-AuNPs is confirmed in Figure 4b, which shows the UV/Vis absorption spectra of all colloids after redispersion of the nanocrystal deposits in water. Interestingly, considering the nonionic nature of IgeSH and α-CD, relatively high negative values of the zeta potential have been measured for IgeS-AuNPs ($\zeta = -17$ mV) and PolyRot-AuNPs ($\zeta = -15$ mV) solutions (Supporting Information). These values are in good agreement with the zeta potential values of gold nanospheres coated by polyethylene glycol polymers with low molecular weights.[21] This suggests that the stabilization of PolyRot-AuNPs within the supercrystals is not only driven by nonionic repulsive interactions between polyrotaxanes, and accordingly to the hydrophobic processes that involve the encapsulation of CDs,[8,9] but also to a substantial electrostatic repulsion between nanocrystals.

In summary, the synthesis of AuNPs stabilized with CD supramolecules proposed herein paves the way for a new method to prepare reusable plasmonic supercrystals, with potential applications in nanoparticle imprinting and sensing. We thus anticipate the use of polyrotaxanes as powerful supramolecular binders, where the separation of the nanocrystals within the supercrystals may be tuned by the length of the molecular axis and the number of macrocycles. Another particularly promising application for this new type of AuNP self-assembly may include the preparation of nanostructures with assembled hollow organic nanocapsules by CD polymerization around the metal core.[22] We are currently focusing on the preparation of new longer thiol-functionalized Igepal surfactants, which could stabilize nanocrystals with different morphologies and sizes (>20 nm) upon addition of α-CD.

Received: June 17, 2014
Revised: September 3, 2014
Published online: September 24, 2014

Keywords: cyclodextrins · gold · nanoparticles · rotaxanes · self-assembly

[1] a) K. J. M. Bishop, C. E. Wilmer, S. Soh, B. A. Grzybowski, *Small* **2009**, *5*, 1600–1630; b) L. R. Macgillivray, G. S. Papaefstathiou, T. Friščić, T. D. Hamilton, D.-K. Bučar, Q. Chu, D. B. Varshney, I. G. Georgiev, *Acc. Chem. Res.* **2008**, *41*, 280–291; c) K. S. Mali, J. Adisoejoso, E. Ghijsens, I. De Cat, S. De Feyter, *Acc. Chem. Res.* **2012**, *45*, 1309–1320.

[2] a) J. A. Theobald, N. S. Oxtoby, M. A. Phillips, N. R. Champness, P. H. Beton, *Nature* **2003**, *424*, 1029–1031; b) M. Cavallini, F. Biscarini, S. León, F. Zerbetto, G. Bottari, D. A. Leigh, *Science* **2003**, *299*, 531; c) A. Ciesielski, P. J. Szabelski, W. Rzìysko, A. Cadeddu, T. R. Cook, P. J. Stang, P. Samorì, *J. Am. Chem. Soc.* **2013**, *135*, 6942–6950.

[3] a) H. Li, D.-X. Chen, Y.-L. Sun, Y. B. Zheng, L.-L. Tan, P. S. Weiss, Y.-W. Yang, *J. Am. Chem. Soc.* **2013**, *135*, 1570–1576; b) R. Freeman, T. Finder, L. Bahshi, R. Gill, I. Willner, *Adv. Mater.* **2012**, *24*, 6416–6421; c) S. Kasera, F. Biedermann, J. J. Baumberg, O. A. Scherman, S. Mahajan, *Nano Lett.* **2012**, *12*, 5924–5928.

[4] a) J.-H. Lee, K.-J. Chen, S.-H. Noh, M. A. Garcia, H. Wang, W.-Y. Lin, H. Jeong, B. J. Kong, D. B. Stout, J. Cheon, H.-R. Tseng, *Angew. Chem. Int. Ed.* **2013**, *52*, 4384–4388; *Angew. Chem.* **2013**, *125*, 4480–4484; b) S. Srivastava, A. Santos, K. Critchley, K.-S. Kim, P. Podsiadlo, K. Sun, J. Lee, C. Xu, G. D. Lilly, S. C. Glotzer, N. A. Kotov, *Science* **2010**, *327*, 1355–1359; c) M.-C. Daniel, D. Astruc, *Chem. Rev.* **2004**, *104*, 293–346.

[5] a) M. Grzelczak, J. Vermant, E. M. Furst, L. M. Liz-Marzán, *ACS Nano* **2010**, *4*, 3591–3605.

[6] a) K. K. Caswell, J. N. Wilson, U. H. F. Bunz, C. J. Murphy, *J. Am. Chem. Soc.* **2003**, *125*, 13914–13915; b) Z. Nie, D. Fava, M. Rubinstein, E. Kumacheva, *J. Am. Chem. Soc.* **2008**, *130*, 3683–3689; c) M. Oh, C. A. Mirkin, *Nature* **2005**, *438*, 651–654; d) N. Goubet, J. Richardi, P.-A. Albouy, M.-P. Pileni, *Adv. Funct. Mater.* **2011**, *21*, 2693–2704; e) R. L. Whetten, M. N. Shafigullin, J. T. Khoury, T. G. Schaaff, I. Vezmar, M. M. Alvarez, A. Wilkinson, *Acc. Chem. Res.* **1999**, *32*, 397–406.

[7] A. Guerrero-Martínez, M. Grzelczak, L. M. Liz-Marzán, *ACS Nano* **2012**, *6*, 3655–3662.

[8] *Molecular Catenanes, Rotaxanes and Knots* (Eds.: J.-P. Sauvage, C. Dietrich-Buchecker), Wiley-VCH, Weinheim, **1999**.

[9] a) A. Harada, M. Kamachi, *Macromolecules* **1990**, *23*, 2821–2823; b) A. Harada, Y. Takashima, H. Yamaguchi, *Chem. Soc. Rev.* **2009**, *38*, 875–882.

[10] K. A. Udachin, L. D. Wilson, J. A. Ripmeester, *J. Am. Chem. Soc.* **2000**, *122*, 12375–12376.

[11] a) A. Guerrero-Martínez, D. Ávila, F. J. Martínez-Casado, J. A. Ripmeester, G. D. Enright, L. De Cola, G. Tardajos, *J. Chem. Phys. B* **2010**, *114*, 11489–11495; b) A. Guerrero-Martínez, T. Montoro, M. Viñas, G. González-Gaitano, G. Tardajos, *J. Phys. Chem. B* **2007**, *111*, 1368–1376.

[12] T. Li, J. Moon, A. A. Morrone, J. J. Mecholsky, D. R. Talham, J. H. Adair, *Langmuir* **1999**, *15*, 4328–4334.

[13] K. Toerne, R. Rogers, R. von Wandruszka, *Langmuir* **2001**, *17*, 6119–6121.

[14] J. Zhao, L. Jensen, J. Sung, S. Zou, G. C. Schatz, R. P. Van Duyne, *J. Am. Chem. Soc.* **2007**, *129*, 7647 – 7656.
[15] G. Wenz, B. H. Han, A. Muller, *Chem. Rev.* **2006**, *106*, 782 – 817.
[16] a) G. Gómez-Graña, J. Pérez-Juste, R. A. Álvarez-Puebla, A. Guerrero-Martínez, L. M. Liz-Marzán, *Adv. Opt. Mater.* **2013**, *1*, 477 – 481; b) T. Ming, X. Kou, H. Chen, T. Wang, H.-L. Tam, K.-W. Cheah, J.-Y. Chen, J. Wang, *Angew. Chem. Int. Ed.* **2008**, *47*, 9685 – 9690; *Angew. Chem.* **2008**, *120*, 9831 – 9836.
[17] T. A. H. Nguyen, M. A. Hampton, A. V. Nguyen, *J. Phys. Chem. C* **2013**, *117*, 4707 – 4716.
[18] C. Hamon, M. Postic, E. Mazari, T. Bizien, C. Dupuis, P. Even-Hernandez, A. Jimenez, L. Courbin, C. Gosse, F. Artzner, V. Marchi-Artzner, *ACS Nano* **2012**, *6*, 4137 – 4146.
[19] E. Tekin, P. J. Smith, U. S. Schubert, *Soft Matter* **2008**, *4*, 703 – 713.
[20] a) R. Klajn, L. Fang, A. Coskun, M. A. Olson, P. J. Wesson, J. F. Stoddart, B. A. Grzybowski, *J. Am. Chem. Soc.* **2009**, *131*, 4233 – 4235; b) M. R. Jones, K. D. Osberg, R. J. MacFarlane, M. R. Langille, C. A. Mirkin, *Chem. Rev.* **2011**, *111*, 3736 – 3827; c) B. Radha, A. J. Senesi, M. N. O'Brien, M. X. Wang, E. Auyeung, B. Lee, C. A. Mirkin, *Nano Lett.* **2014**, *14*, 2162 – 2167.
[21] a) K. Rahme, L. Chen, R. G. Hobbs, M. A. Morris, C. O'Driscoll, J. D. Holmes, *RSC Adv.* **2013**, *3*, 6085 – 6094; b) S. D. Perrault, W. C. W. Chan, *J. Am. Chem. Soc.* **2009**, *131*, 17042 – 17043.
[22] Y.-L. Wu, J. Li, *Angew. Chem. Int. Ed.* **2009**, *48*, 3842 – 3845; *Angew. Chem.* **2009**, *121*, 3900 – 3903.

